haematologica
Journal of the Ferrata Storti Foundation

Metallothionein 1 mediates growth and survival of *Dnmt3a;Npm1*-mutant acute myeloid leukemia

by Patricia A. Colom Diaz, Jayna J. Mistry, Kira A. Young, Chih-Hsing Chou, Nathan Boyer, Ross L. Levine, Nathan Salomonis , H. Leighton Grimes and Jennifer J. Trowbridge

Received: February 21, 2025.
Accepted: August 4, 2025.

Citation: Patricia A. Colom Diaz, Jayna J. Mistry, Kira A. Young, Chih-Hsing Chou, Nathan Boyer, Ross L. Levine, Nathan Salomonis , H. Leighton Grimes and Jennifer J. Trowbridge.
Metallothionein 1 mediates growth and survival of Dnmt3a;Npm1-mutant acute myeloid leukemia.
Haematologica. 2025 Aug 14. doi: 10.3324/haematol.2025.287662 [Epub ahead of print]

Metallothionein 1 mediates growth and survival of *Dnmt3a;Npm1*-mutant acute myeloid leukemia

Patricia A. Colom Díaz[1], Jayna J. Mistry[1], Kira A. Young[1], Chih-Hsing Chou[2], Nathan Boyer[1], Ross L. Levine[3], Nathan Salomonis[4,5], H. Leighton Grimes[5], Jennifer J. Trowbridge[1*]

[1]The Jackson Laboratory, Bar Harbor, ME, USA
[2]Division of Immunobiology, Cincinnati Children's Hospital Medical Center (CCHMC), Cincinnati, OH, USA
[3]Memorial Sloan Kettering Cancer Center, New York, NY, USA
[4]Division of Biomedical Informatics, CCHMC, Cincinnati, OH, USA
[5]Division of Experimental Hematology and Cancer Biology, CCHMC, Cincinnati, OH, USA

*Corresponding author:
Jennifer Trowbridge, The Jackson Laboratory
600 Main Street, Bar Harbor, ME
Jennifer.trowbridge@jax.org

Author Contributions

P.A.C.D., J.J.M., K.A.Y., and J.J.T. designed the study with contributions from C.-H.C., N.S., and H.L.G. on experimental design. P.A.C.D., J.J.M., K.A.Y., and C.-H.C. collected data. P.A.C.D., J.J.M., C.-H.C., N.B., N.S., and J.J.T. analyzed data. P.A.C.D., J.J.M., K.A.Y., R.L.L., N.S., H.L.G. and J.J.T. interpreted data. J.J.M. and J.J.T. drafted the article. All authors edited and reviewed the final version of the manuscript.

Competing Interests Disclosure

R.L.L. is on the Supervisory board of Qiagen (compensation/equity), a co-founder/board member at Ajax (equity), and is a scientific advisor to Mission Bio, Kurome, Anovia, Bakx, Syndax, Scorpion, Zentalis, Auron, Prelude, and C4 Therapeutics; for each of these entities he receives equity/compensation. He has received research support from the Cure Breast Cance Foundation, Calico, Zentalis and Ajax, and has consulted for Jubilant, Goldman Sachs, Incyte, Astra Zeneca and Janssen. J.J.T. has previously received research support from H3 Biomedicine, Inc., and patent royalties from Fate Therapeutics. All other authors declare no competing interests.

Acknowledgements

The authors thank all members of the Trowbridge lab for experimental assistance, input, and critical discussions, particularly Maria Telpoukhovskaia, Griffin Nye and Xiurong Cai. This work was supported by U01AG077925 (J.J.T. and R.L.L.), R01DK118072 (J.J.T.), R01AG069010 (J.J.T.), P30CA034196 (J.J.T.), RC2DK122376 (H.L.G.), R01CA284595 (H.L.G.), R01HL122661 (H.L.G.), R01CA253981 (H.L.G.), and the Edward P. Evans Foundation (J.J.T.). J.J.T. was supported by a Leukemia and Lymphoma Society Scholar award. J.J.M. was supported by a Leukemia & Lymphoma Society Career Development Program Fellow Award and The Jackson Laboratory Scholar Award.

Data Availability

Single cell RNA-seq and bulk RNA-seq data generated in this study are deposited in the NCBI Gene Expression Omnibus (GEO) under accession numbers GSE277963 (reviewer token: kjkniqqstlwvzsl) and GSE262264.

Acute myeloid leukemia (AML) is an aggressive malignancy associated with poor outcomes[1]. Deregulation of transcriptional programs resulting in malignant cell self-renewal and impaired differentiation is a molecular hallmark of AML[2]. Thus, targeting transcriptional dependencies of AML is a promising approach to impair cell-intrinsic mechanisms sustaining this malignancy. Here, we investigated transcriptional patterns across cell states utilizing a sequentially inducible model of AML[3] combining two of the most common and frequently co-mutated genes in cytogenetically normal human *de novo* AML; DNA methyltransferase 3A (*DNMT3A*) and nucleophosmin *(NPM1*)[4].

We performed single-cell RNA-seq and cellHarmony analysis[5] of primitive c-Kit^{+} cells enriched using magnetic-activated cell sorting from four primary *Dnmt3a*$^{R878H/+}$ *Npm1*$^{cA/+}$ (*Dnmt3a;Npm1*-mutant) AML spleen samples[3] (**Figure 1A**) (GSE277963, reviewer token: kjkniqqstlwvzsl). All mouse studies were approved by The Jackson Laboratory's Institutional Animal Care and Use Committee (IACUC). We integrated this data with a healthy hematopoietic cell atlas of 87 cell states spanning all major bone marrow (BM) lineages. This atlas includes rare and transitional cell states (**Supplementary Figure 1A**). As this atlas excluded predominant hematopoietic and stromal cell populations in the spleen, we included distinct cell states identified in spleen single-cell RNA-Seq for the annotation of our datasets (**Supplementary Figure 1B, C**). The most primitive cell populations found in all *Dnmt3a;Npm1*-mutant AML samples were multi-lineage primed MultiLin-2 (ML-2) progenitors (**Supplementary Figure 1D**). Using differential gene expression analysis of *Dnmt3a;Npm1*-mutant AML progenitors compared to their normal BM counterparts, the transcript *Mt1* was the top gene significantly increased in expression across all samples (**Figure 1B, Supplementary Figure 2**). We compared *Mt1* expression in MultiLin-2 cells profiled from eight different mouse models harboring preleukemic mutations[6], wild-type BM controls, and *Dnmt3a;Npm1*-mutant AML mice from this study (2-4 biological replicates per genotype). We observed that increased expression of *Mt1* was highly specific to *Dnmt3a;Npm1*-mutant AML and is not induced by individual mutations in *Dnmt3a* or *Npm1* alone (**Figure 1C, D**).

Metallothionein 1 (Mt1) is a low molecular weight, cysteine-rich intracellular protein that can bind to both essential and toxic metals[7]. To identify potential role(s) of *Mt1* in *Dnmt3a;Npm1*-mutant AML, we performed knockout of *Mt1* by electroporation of Cas9-sgRNA complexes (RNPs) into primary *Dnmt3a;Npm1*-mutant AML cells. We began by pooling three sgRNAs targeting the *Mt1* locus (**Figure 2A**). With this approach, >80% of cells were confirmed by sequencing to have an INDEL at the targeted region of the *Mt1* locus (**Figure 2B**). We performed differential expression analysis using RNA-seq from three independent replicates compared to control *Dnmt3a;Npm1*-mutant AML cells electroporated with Cas9 but no sgRNA (GSE262264). From this analysis, 256 genes were increased (ex. *Cpa3, Ctla2a, Tpsb2, Cma1*) and 89 genes decreased (ex. *Mt1, Ccn2, Aebp1, Col5a2*) with a significance cutoff of $p < 0.05$ (**Figure 2C**). Gene set enrichment analysis revealed that knockout of *Mt1* reduced the expression of cell cycling signatures and increased expression of genes signatures related to differentiation, pyroptosis, and oxidative stress (**Figure 2D**). Based on these data, we hypothesized that knockout of *Mt1* would promote cell death and reduced cell cycling of primary *Dnmt3a;Npm1*-mutant AML cells. To test this, we evaluated cell proliferation and growth of *Mt1* knockout *Dnmt3a;Npm1*-mutant AML cells relative to an expanded set of negative control conditions including no sgRNA, scrambled sgRNA, and sgRNA targeting of the non-essential *Rosa26* locus **(Figure 2E and F)**. Compared to these negative controls, knockout of *Mt1* in primary *Dnmt3a;Npm1*-mutant AML cells resulted in decreased proliferation assessed by Ki67 staining (**Figure 2G**) and reduced growth in 5-day cultures (**Figure 2H**). To assess

the rigor of sgRNA-mediated knockout of *Mt1*, we tested individual sgRNAs which each achieved ~10-40% knockout efficiency (**Figure 2I**). These individual sgRNAs were sufficient to impair growth of *Dnmt3a;Npm1*-mutant AML cells in 5-day cultures to a level comparable to knockout of *Pcna* (**Figure 2J**). We utilized *Pcna* as a positive control which is an essential component of the DNA replication machinery known to be a common cellular dependency.

To evaluate how knockout of *Mt1* impacts leukemogenicity *in vivo*, sublethally irradiated recipient mice ($CD45.1^+$) were transplanted with *Mt1*-knockout or control primary *Dnmt3a;Npm1*-mutant AML cells ($CD45.2^+$) (**Figure 3A**). At 4 weeks post-transplant, we found significantly fewer AML ($CD45.2^+$) cells detected in the recipients of *Mt1*-knockout AML compared to negative controls (**Figure 3B**). Mice receiving *Mt1*-knockout AML cells also survived significantly longer than mice transplanted with control AML cells (**Figure 3C**). In moribund recipient mice, the proportion of AML cells retaining *Mt1* knockout was variable (**Figure 3D**), and survival of individual recipient mice positively correlated with the proportion of *Mt1*-knockout AML cells remaining (**Figure 3E**), demonstrating that knockout of *Mt1* reduced the leukemogenicity of *Dnmt3a;Npm1*-mutant AML *in vivo*.

In humans, there are eight functional MT1 isoforms and the transcript levels of *MT1F*, *MT1G*, *MT1H* and *MT1X* have been shown to be increased in human AML compared to normal BM samples in the ONCOMINE database[8]. In the *DNMT3A;NPM1*-mutant human AML cell line, OCI-AML3, we observed significantly increased expression of the isoform *MT1G* compared to normal BM cells and the human *DNMT3A*-mutant *NPM1*-wildtype AML cell line OCI-AML2 (**Figure 3F**). We performed knockout of *MT1G* in OCI-AML2 and OCI-AML3 cells by electroporation of Cas9 RNPs using a sgRNA targeting exon 1, achieving a similar knockout efficiency in both cell lines (**Figure 3G**). In OCI-AML2 cells, knockout of *MT1G* did not impact cell growth in culture unlike the positive control *PCNA* which significantly decreased viability (**Figure 3H**). In contrast, in OCI-AML3 cells, knockout of *MT1G* decreased cell counts in culture to a similar level as the positive control *PCNA* (**Figure 3I**). These data support that in human AML cells, similar to what we see in mouse *Dnmt3a;Npm1*-mutant AML cells, increased expression and dependency of *MT1G* occurs in *DNMT3A;NPM1*-mutant AML which is not induced by an individual mutation in *DNMT3A* alone.

In mouse hematopoietic stem cells (HSCs), the *Mt1* locus is methylated by Dnmt3a as evidenced by *Mt1* hypomethylation in *Dnmt3a*-knockout HSCs using whole-genome bisulfite sequencing [9, 10]. However, *Mt1* is not increased in expression in *Dnmt3a*-knockout or mutant HSCs [9, 10], indicating that cooperativity with an *Npm1* mutation and transformation to AML are prerequisites for observing transcriptional upregulation of *Mt1*. Understanding the function of Mt1 in AML progenitor cells requires further study. It is known that metallothionein protects cells against radiation and chemotherapeutic agents by virtue of its free radical scavenging property[11, 12]. In newly diagnosed pediatric AML, metallothionein expression is associated with increased risk of relapse[13]. Our study expands on this literature by demonstrating that mouse and human *Dnmt3a;Npm1*-mutant AML is sensitive to loss of metallothionein expression. A current limitation is that the only mouse model available is a dual *Mt1* and *Mt2* germline knockout[14] which is a barrier to ascertaining the role of Mt1 in normal HSCs, and no small molecule inhibitors targeting MT1 or MT1G are available to our knowledge. Therefore, development of new tools and methodologies are needed to better understand the role of metal toxicity and oxidative stress in AML risk and relapse.

References

1. Kurzer JH, Weinberg OK. Updates in molecular genetics of acute myeloid leukemia. Semin Diagn Pathol. 2023;40(3):140-151.
2. Khan I, Eklund EE, Gartel AL. Therapeutic Vulnerabilities of Transcription Factors in AML. Mol Cancer Ther. 2021;20(2):229-237.
3. Loberg MA, Bell RK, Goodwin LO, et al. Sequentially inducible mouse models reveal that Npm1 mutation causes malignant transformation of Dnmt3a-mutant clonal hematopoiesis. Leukemia. 2019;33(7):1635-1649.
4. Cancer Genome Atlas Research Network, Ley TJ, Miller C, et al. Genomic and epigenomic landscapes of adult de novo acute myeloid leukemia. N Engl J Med. 2013;368(22):2059-2074.
5. DePasquale EAK, Schnell D, Dexheimer P, et al. cellHarmony: cell-level matching and holistic comparison of single-cell transcriptomes. Nucleic Acids Res. 2019;47(21):e138.
6. Isobe T, Kucinski I, Barile M, et al. Preleukemic single-cell landscapes reveal mutation-specific mechanisms and gene programs predictive of AML patient outcomes. Cell Genom. 2023;3(12):100426.
7. Cherian MG, Jayasurya A, Bay BH. Metallothioneins in human tumors and potential roles in carcinogenesis. Mutat Res. 2003;533(1-2):201-209.
8. Xin X, Xu Z, Wei J, Zhang Y. MiR-376a-3p increases cell apoptosis in acute myeloid leukemia by targeting MT1X. Cancer Biol Ther. 2022;23(1):234-242.
9. Jeong M, Park HJ, Celik H, et al. Loss of Dnmt3a Immortalizes Hematopoietic Stem Cells In Vivo. Cell Rep. 2018;23(1):1-10.
10. Jeong M, Sun D, Luo M, et al. Large conserved domains of low DNA methylation maintained by Dnmt3a. Nat Genet. 2014;46(1):17-23.
11. Lazo JS, Kuo SM, Woo ES, Pitt BR. The protein thiol metallothionein as an antioxidant and protectant against antineoplastic drugs. Chem Biol Interact. 1998;111-112:255-262.
12. Shibuya K, Nishimura N, Suzuki JS, Tohyama C, Naganuma A, Satoh M. Role of metallothionein as a protective factor against radiation carcinogenesis. J Toxicol Sci. 2008;33(5):651-655.
13. Sauerbrey A, Zintl F, Hermann J, Volm M. Multiple resistance mechanisms in acute nonlymphoblastic leukemia (ANLL). Anticancer Res. 1998;18(2B):1231-1236.
14. Masters BA, Kelly EJ, Quaife CJ, Brinster RL, Palmiter RD. Targeted disruption of metallothionein I and II genes increases sensitivity to cadmium. Proc Natl Acad Sci U S A. 1994;91(2):584-588.

Figure Legends

Figure 1. *Mt1* is a top upregulated gene in mouse *Dnmt3a*;*Npm1*-mutant AML progenitor cells. (**A**) Experimental design for single-cell RNA-seq. Created in BioRender. Trowbridge, J. (2025) https://BioRender.com/nzoaehw (**B**) Volcano plots of differential gene expression in Multi-Lin-2 cells from *Dnmt3a*;*Npm1*-mutant AMLs versus CellHarmony reference. (**C**) Violin plot of *Mt1* expression in Multi-Lin-2 cells from eight previously reported mouse models harboring pre-leukemic mutations[6], control wild-type BM and *Dnmt3a*;*Npm1*-mutant AML mice from this study (2-4 biological replicates). Individual dots are single-cell log-transformed normalized expression values. (**D**) Dotplot of fold change in *Mt1* expression (log2) in Multi-Lin-2 cells. The size and color of each dot corresponds to the -log10 p-value of a Welch's *t*-test (two-sided, unequal variance assumption) comparing log-transformed normalized expression values in mutants vs. wild-type control BM.

Figure 2. Knockout of *Mt1* impairs cell growth of mouse *Dnmt3a*;*Npm1*-mutant AML cells. (**A**) Experimental design for Cas9-mediated *Mt1* knockout. Created in BioRender. Trowbridge, J. (2025) https://BioRender.com/hobbbyh (**B**) Proportion of *Dnmt3a*;*Npm1*-mutant AML cells with indels detected at the *Mt1* locus. Each dot represents a biological replicate. (**C**) Volcano plot showing significantly differentially expressed genes in *Mt1* knockout *Dnmt3a*;*Npm1*-mutant AML cells versus control *Dnmt3a*;*Npm1*-mutant AML cells. n = 3 biological replicates per condition. *Mt1* is denoted in red. (**D**) Normalized enrichment scores of gene signatures enriched in *Mt1* knockout compared to control *Dnmt3a*;*Npm1*-mutant AML cells. (**E-F**) Proportion of AML cells with indels detected at the (**E**) *Rosa26* or (**F**) *Mt1* locus. Each dot represents a biological replicate. (**G**) Frequency of $Ki67^+$ cells in control and *Mt1* knockout *Dnmt3a*;*Npm1*-mutant AML cells. Dots represent individual biological replicates (n = 3). $^{**}p < 0.01$, $^{***}p < 0.001$ by one-way ANOVA with Tukey's multiple comparisons test. (**H**) Fold change in viable cell count after 5 day culture of control and *Mt1* knockout *Dnmt3a*;*Npm1*-mutant AML cells. Dots represent individual biological replicates (n = 4-6). $^{**}p < 0.01$, $^{***}p < 0.001$ by one-way ANOVA with Dunnett's multiple comparisons test. (**I**) Proportion of AML cells with indels detected at the *Mt1* locus. (**J**) Fold change in viable cell count after 5 day culture of control and *Mt1* knockout *Dnmt3a*;*Npm1*-mutant AML cells. Dots represent individual biological replicates (n = 3). $^{*}p < 0.05$, $^{****}p < 0.0001$ by one-way ANOVA with Dunnett's multiple comparisons test.

Figure 3. Knockout of *Mt1* reduces growth of mouse *Dnmt3a*;*Npm1*-mutant AML cells *in vivo* and the human *DNMT3A;NPM1*-mutant AML cell line OCI-AML3. (**A**) Experimental design for *in vivo* assays. Created in BioRender. Trowbridge, J. (2025) https://BioRender.com/viw75wf (**B**) Frequency of control or *Mt1* knockout *Dnmt3a*;*Npm1*-mutant AML ($CD45.2^+$) cells in the peripheral blood of transplanted recipient mice at 4 weeks post-transplant. Each dot represents one recipient mouse (n = 5). $^{*}p < 0.05$, $^{**}p < 0.01$ by one-way ANOVA with Fisher's LSD. (**C**) Survival curve of mice transplanted with control and *Mt1* knockout *Dnmt3a*;*Npm1*-mutant AML cells (n = 5 per condition). $^{**}p < 0.01$ by log-rank (Mantel-Cox) test. (**D**) Proportion of AML cells at mouse harvest with INDELs detected at the *Mt1* locus. Each dot represents an individual mouse. (**E**) Correlation between mouse survival and *Mt1* knockout detected at harvest for mice transplanted with *Mt1* knockout *Dnmt3a*;*Npm1*-mutant AML cells. Each dot represents an individual mouse. (**F**) Relative expression of *MT1G* in OCI-AML2 and OCI-AML3 cells relative to wild-type BM $CD34^+$ hematopoietic stem and progenitor cells. Dots represent biological replicates (n = 3). $^{***}p < 0.001$ by one-way ANOVA with Tukey's multiple comparisons test.

(**G**) Proportion of AML cells with indels detected at the *Mt1G* locus. (**H-I**) Viable cell counts after 3-day culture of (**H**) OCI-AML2 and (**I**) OCI-AML3 cells with *MT1G* knockout compared to controls. Dots represent independent replicate experiments ($n = 3$). **$p < 0.01$, ***$p < 0.001$ by one-way ANOVA with Dunnett's multiple comparisons test.

Figure 1

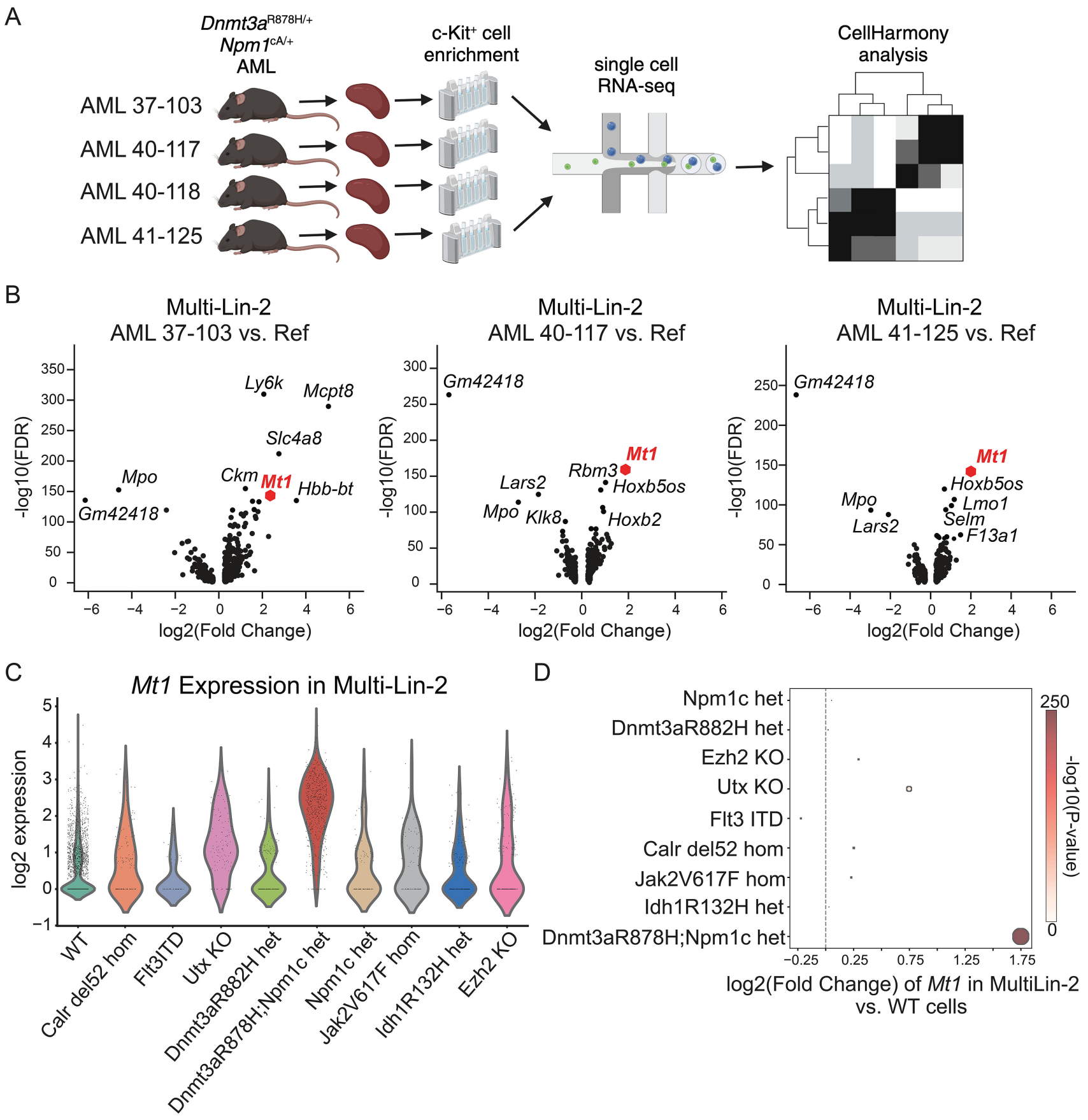
A
Dnmt3a R878H/+
Npm1 cA/+
AML
AML 37-103
AML 40-117
AML 40-118
AML 41-125
c-Kit+ cell enrichment
single cell RNA-seq
CellHarmony analysis
B
Multi-Lin-2
AML 37-103 vs. Ref
Multi-Lin-2
AML 40-117 vs. Ref
Multi-Lin-2
AML 41-125 vs. Ref
-log10(FDR)
log2(Fold Change)
Ly6k
Mcpt8
Slc4a8
Mpo
Ckm
Mt1
Hbb-bt
Gm42418
Rbm3
Lars2
Hoxb5os
Mpo
Klk8
Hoxb2
Lmo1
Selm
F13a1
C
Mt1 Expression in Multi-Lin-2
log2 expression
WT
Calr del52 hom
Flt3ITD
Utx KO
Dnmt3aR882H het
Dnmt3aR878H;Npm1c het
Npm1c het
Jak2V617F hom
Idh1R132H het
Ezh2 KO
D
Npm1c het
Dnmt3aR882H het
Ezh2 KO
Utx KO
Flt3 ITD
Calr del52 hom
Jak2V617F hom
Idh1R132H het
Dnmt3aR878H;Npm1c het
-log10(P-value)
log2(Fold Change) of Mt1 in MultiLin-2 vs. WT cells

Figure 2

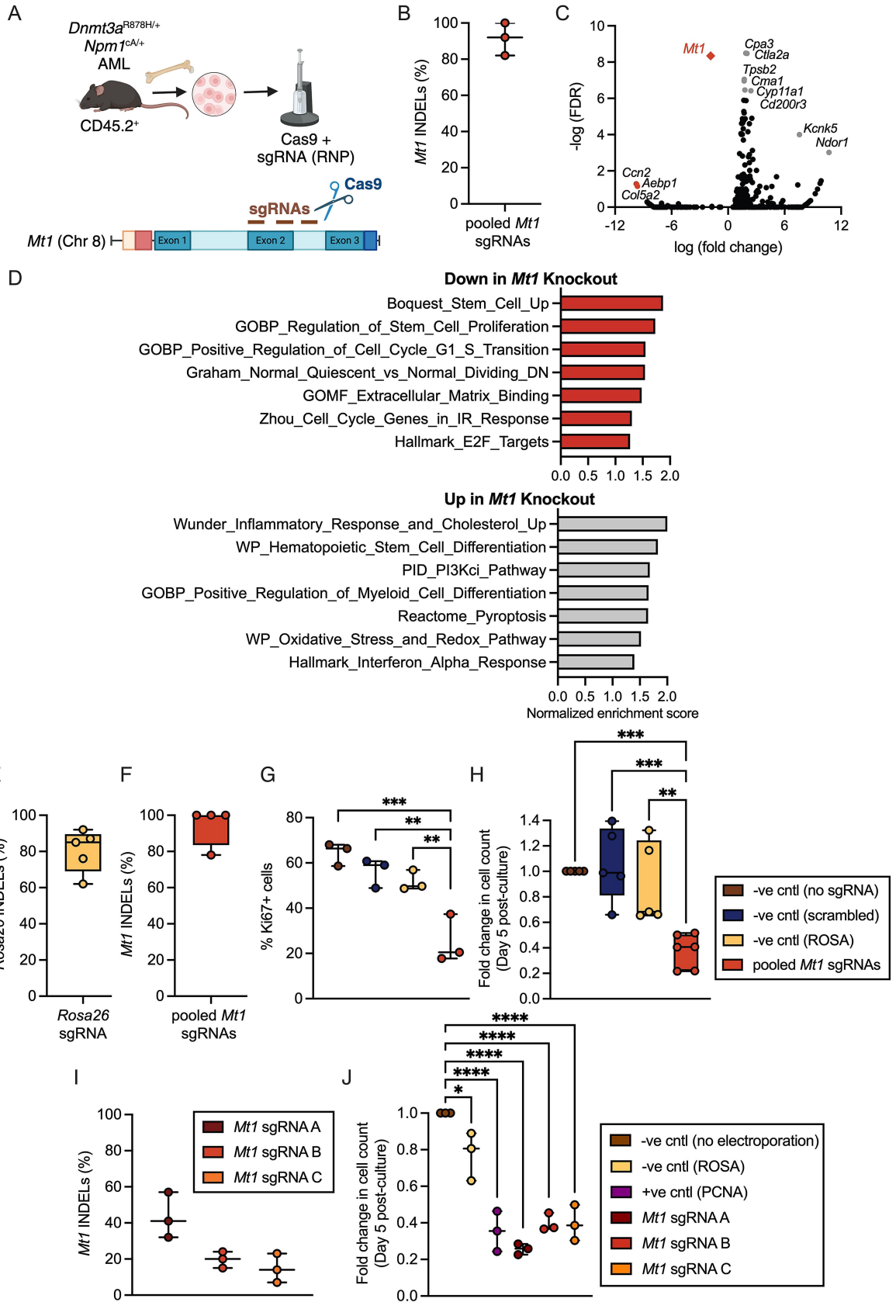
A
Dnmt3a R878H/+
Npm1 cA/+
AML
CD45.2+
Cas9 +
sgRNA (RNP)
Cas9
sgRNAs
Mt1 (Chr 8)
Exon 1
Exon 2
Exon 3
B
Mt1 INDELs (%)
pooled Mt1
sgRNAs
C
-log (FDR)
log (fold change)
Mt1
Cpa3
Ctla2a
Tpsb2
Cma1
Cyp11a1
Cd200r3
Kcnk5
Ndor1
Ccn2
Aebp1
Col5a2
D
Down in Mt1 Knockout
Boquest_Stem_Cell_Up
GOBP_Regulation_of_Stem_Cell_Proliferation
GOBP_Positive_Regulation_of_Cell_Cycle_G1_S_Transition
Graham_Normal_Quiescent_vs_Normal_Dividing_DN
GOMF_Extracellular_Matrix_Binding
Zhou_Cell_Cycle_Genes_in_IR_Response
Hallmark_E2F_Targets
Up in Mt1 Knockout
Wunder_Inflammatory_Response_and_Cholesterol_Up
WP_Hematopoietic_Stem_Cell_Differentiation
PID_PI3Kci_Pathway
GOBP_Positive_Regulation_of_Myeloid_Cell_Differentiation
Reactome_Pyroptosis
WP_Oxidative_Stress_and_Redox_Pathway
Hallmark_Interferon_Alpha_Response
Normalized enrichment score
E
Rosa26 INDELs (%)
Rosa26
sgRNA
F
Mt1 INDELs (%)
pooled Mt1
sgRNAs
G
% Ki67+ cells
H
Fold change in cell count
(Day 5 post-culture)
-ve cntl (no sgRNA)
-ve cntl (scrambled)
-ve cntl (ROSA)
pooled Mt1 sgRNAs
I
Mt1 INDELs (%)
Mt1 sgRNA A
Mt1 sgRNA B
Mt1 sgRNA C
J
Fold change in cell count
(Day 5 post-culture)
-ve cntl (no electroporation)
-ve cntl (ROSA)
+ve cntl (PCNA)
Mt1 sgRNA A
Mt1 sgRNA B
Mt1 sgRNA C

Figure 3

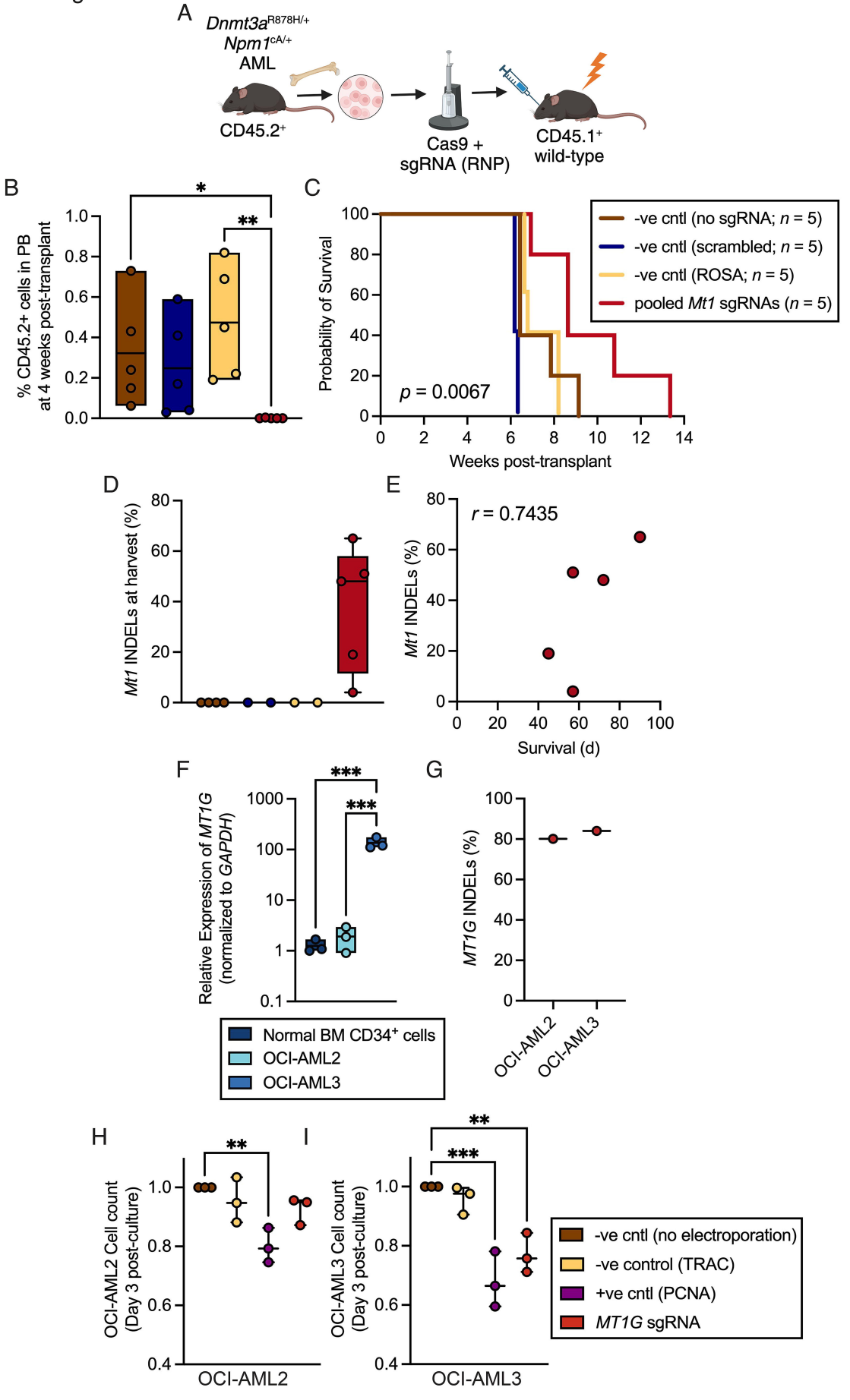
A
Dnmt3a R878H/+
Npm1 cA/+
AML
CD45.2+
Cas9 +
sgRNA (RNP)
CD45.1+
wild-type
B
% CD45.2+ cells in PB
at 4 weeks post-transplant
C
Probability of Survival
p = 0.0067
Weeks post-transplant
-ve cntl (no sgRNA; n = 5)
-ve cntl (scrambled; n = 5)
-ve cntl (ROSA; n = 5)
pooled Mt1 sgRNAs (n = 5)
D
Mt1 INDELs at harvest (%)
E
r = 0.7435
Mt1 INDELs (%)
Survival (d)
F
Relative Expression of MT1G
(normalized to GAPDH)
Normal BM CD34+ cells
OCI-AML2
OCI-AML3
G
MT1G INDELs (%)
OCI-AML2
OCI-AML3
H
OCI-AML2 Cell count
(Day 3 post-culture)
I
OCI-AML3 Cell count
(Day 3 post-culture)
-ve cntl (no electroporation)
-ve control (TRAC)
+ve cntl (PCNA)
MT1G sgRNA

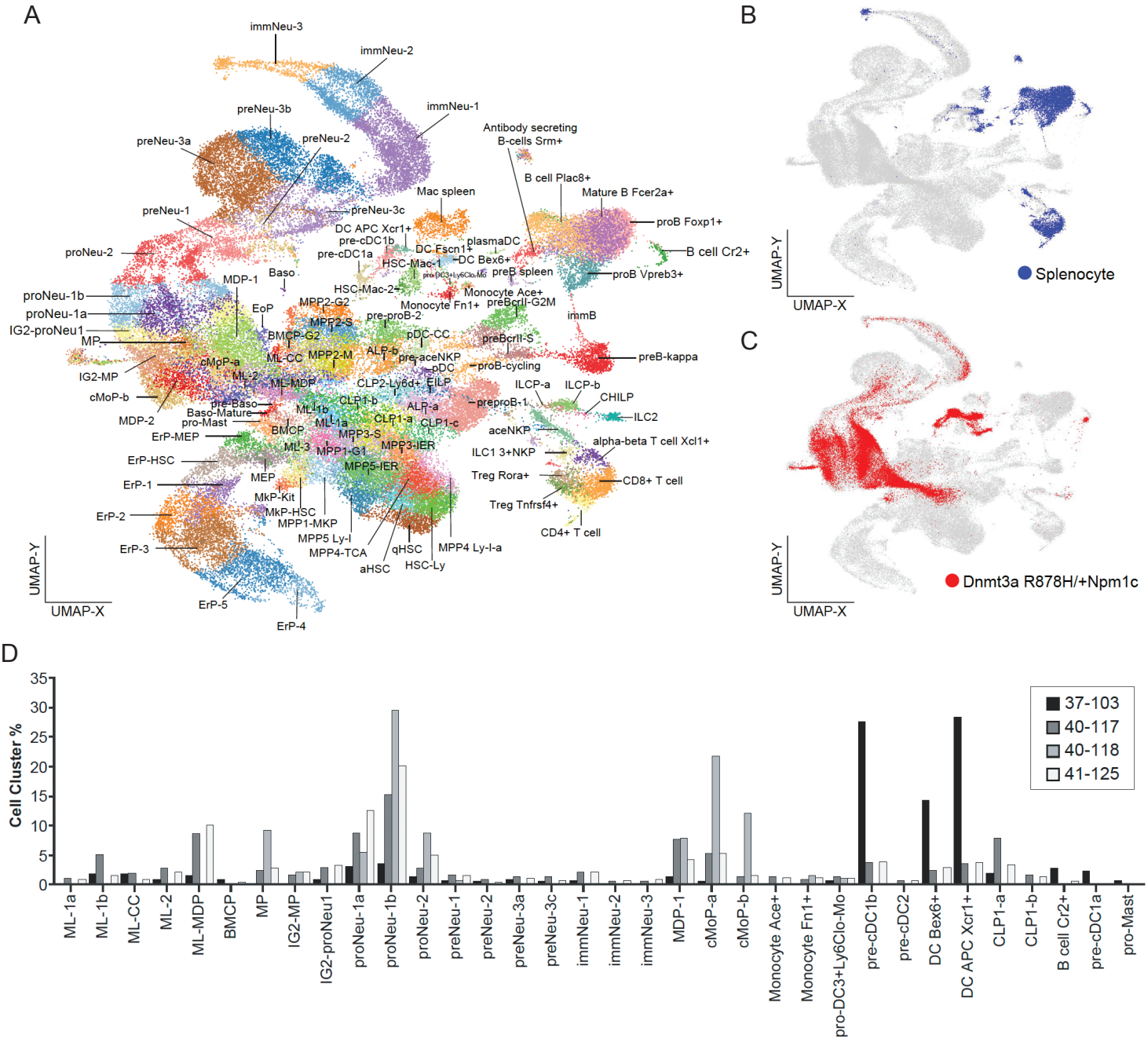

Supplementary Figure 1. Integrated comparison of bone marrow and spleen cells with *Dnmt3a;Npm1*-mutant AML progenitors. UMAP plots of cellHarmony-defined progenitor and mature cell types in (**A**) healthy bone marrow progenitors and splenocytes, (**B**) splenocytes only and (**C**) projected *Dnmt3a;Npm1*-mutant progenitors. (**D**) The proportion of progenitor and mature cell types within a c-Kit^{+} enriched fraction of 4 primary *Dnmt3a;Npm1*-mutant AML samples.

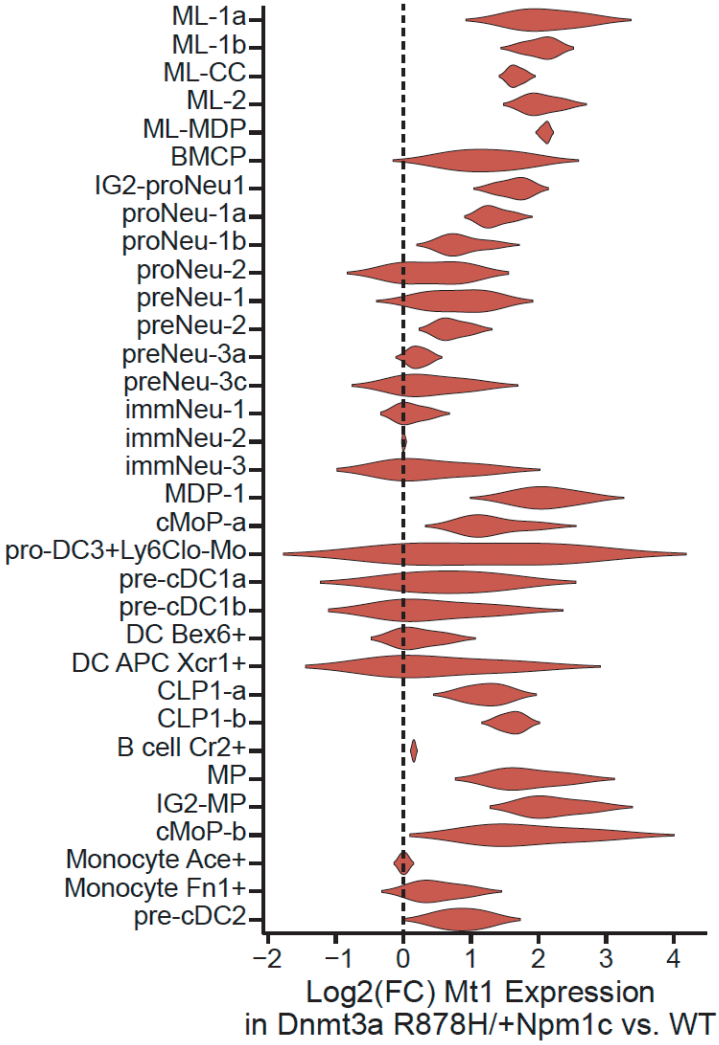

Supplementary Figure 2. Log2 fold change in *Mt1* expression in all cell types identified in c-Kit+ *Dnmt3a;Npm1*-mutant AML samples relative to the respective reference population. The vertical dotted line represents no change in expression.